G Model
CIRP-1498; No. of Pages 4
ARTICLE IN PRESS
CIRP Annals - Manufacturing Technology xxx (2016) xxx–xxx
Contents lists available at ScienceDirect
CIRP Annals - Manufacturing Technology
journal homepage: http://ees.elsevier.com/cirp/default.asp

A mechanics-based predictive model for chip breaking in metal machining and its validation

S. Buchkremer [a,*], J. Schoop [b]

[a] Laboratory for Machine Tools and Production Engineering (WZL), RWTH Aachen University, Germany
[b] Institute for Sustainable Manufacturing (ISM), University of Kentucky, USA

ARTICLE INFO

Article history:
Submitted by I.S. Jawahir (1), University of Kentucky, USA

Keywords:
Chip
Fracture analysis
Chip breakage

ABSTRACT

In metal cutting, effective chip breaking enables efficient chip removal, prevents workpiece and tool damage, and provides operational safety. Currently available cutting tool insert designs often neglect the underlying physics of chip breaking process governed by ductile fracture on the chip free-surface. This paper presents a predictive model for chip breaking in turning operations, which combines a mechanics-based model, utilizing a ductile fracture criterion, with a finite element model. Experimental validation on aluminum alloy *AA7075-T6511* and brass *CuZn38As* shows that the impacts of the tool and process parameters on chip breakability could be accurately predicted without prior knowledge of the ductile material properties.

1. Introduction

In metal cutting, the process stability and efficiency are evaluated by machinability criteria, including tool-wear, surface integrity and chip-form. When machining ductile materials in highly automated production systems, the chip-form may dominate the machinability: unbroken chips may scratch the machined surface, hinder automated chip removal, or interfere in the tool–workpiece interface, which may yield to tool breakage, poor surface quality, etc. [1,2]. Despite the high industrial relevance of chip breaking, the established cutting design methodologies and process plans still largely follow only empirical and "trial and error" approaches.

Extensive past experimental investigations have identified and empirically-modeled the interrelationships among the tool and process parameters, and chip breakability for different materials [3,4]. The experimental understanding of the chip breaking process enabled the abstraction toward physically-relevant technological quantities including the tool–chip contact length, thermal work material properties and the chip up-/side-curling behavior [5–7]. Also, the cyclic nature of the chip breaking process has been studied. It has been shown that after its formation, the chip flows over the tool rake face and curls away. Eventually its free-end contacts either the workpiece surface or the tool flank face, and due to this contact a bending moment develops in the chip, thus resulting in chip breaking [8].

Many analytical models assumed that the bending phase ends as soon as a critical deformation is exceeded on the chip's free surface. Nakayama [9] proposed a model of the chip strain increase ϵ during the bending phase in orthogonal cutting, which is shown as follows:

$$\epsilon = \frac{h'}{2} \cdot \left(\frac{1}{r_{u1}} - \frac{1}{r_{u2}} \right) \quad (1)$$

where the up-curl radius at the beginning of bending r_{u1} expands to r_{u2} and h' denotes the chip thickness. Over the years, many authors adopted, and modified, Nakayama's equation, and even applied it to 3D machining processes [10,11]. However, Eq. (1) does not consider the underlying physics of material failure, to which chip breakage is attributed. Athavale and Strenkowski were among the first to correlate chip breakage with the accumulation of ductile damage, which yields to final fracture at the end of the chip bending phase [12]. Essig's scanning electron microscopical investigations of broken chips of *AISI 1045* steel reveal the typical honeycomb-like fracture surfaces, which indicate ductile material fracture [13]. Ductile fracture is governed by the formation, growth and coalescence of voids at the chip breakage location. The critical strain at ductile fracture is a function of the stress state in terms of the stress triaxiality η and Lode parameter Θ, the temperature T and the strain-rate $\dot{\epsilon}$, as described, for example, by Johnson and Cook [14], as well as Bai and Wierzbicki [15]. In this regard, the triaxiality can be interpreted as a measure for the multi-axiality of the stress state, while the Lode parameter reflects the loading direction (i.e., compression, shear, tension). Klocke et al. [16] applied the Johnson–Cook fracture model, and Buchkremer et al. [17] modified the Bai–Wierzbicki model for the 3D FE simulation of chip breakage. However, these approaches do not provide a predictive capability for designing cutting tools and processes.

In this paper, we summarize the development, application and validation of a systematic predictive methodology of tool and process design for stable chip breakage in metal cutting. A model of

* Corresponding author.
E-mail address: s.buchkremer@wzl.rwth-aachen.de (S. Buchkremer).

http://dx.doi.org/10.1016/j.cirp.2016.04.089
0007-8506/© 2016 CIRP.

ductile fracture is embedded, which takes into account the stress triaxiality, Lode parameter and temperature. The proposed calibration methodology incorporates the loading path impact. In an experimental validation it is shown that the methodology enables predictions of the impacts of tool and process parameters on chip breaking without prior knowledge of the ductile material properties necessary. The validation is carried out on high strength aluminum alloy *AA7075-T6511* and low-leaded brass *CuZn38As*, for which the governing fracture mechanisms were investigated in detail.

First, the turning experiments and characterization of fracture mechanisms are presented, followed by the presentation of the chip breakage modeling and a fracture mechanics interpretation.

2. Turning experiments

2.1. Materials and experimental set-up

External longitudinal turning tests were performed on aluminum alloy *AA7075-T6511* and brass *CuZn38As*. Table 1 gives micrographs and some mechanical properties of both work materials.

Table 1
Micrographs and some mechanical properties of aluminum alloy *AA7075-T6511* and brass *CuZn38As*.

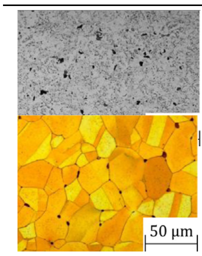

Aluminum alloy *AA7075-T6511*			
Mechanical properties			
Yield point $R_{p0.2}$	Tensile strength R_m	Elongation A_f	Density ρ
535 MPa	585 MPa	9.66%	2810 kg/m^3
Brass *CuZn38As*			
Mechanical properties			
Yield point $R_{p0.2}$	Tensile strength R_m	Elongation A_f	Density ρ
293 MPa	388 MPa	31.2%	8410 kg/m^3

The workpieces were obtained as bars with diameters of 40 mm for *AA7075-T6511*, and 30 mm for *CuZn38As*. A Weisser FrontorM1 CNC lathe was used with no coolant or lubricant. Three tools (CNMG12040X) with varying rake face geometries and varying standard tool corner radii were utilized under different cutting edge angles, see Table 2. The chip-forms were investigated at different feeds and depths of cut for both materials as presented in Section 3.2. The cutting speeds were kept constant at 200 m/min for *AA7075-T6511* and 150 m/min for *CuZn38As*, respectively.

Table 2
Tool inserts and applied tool angles.

Tool T1 (finishing)	T2 (semi roughing)	T3 (semi roughing)

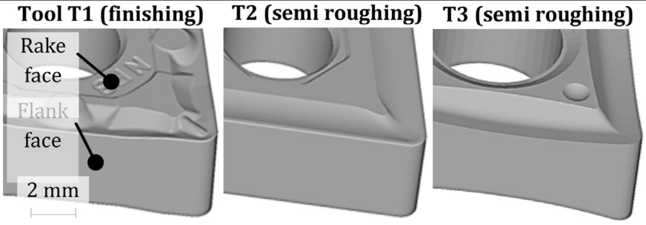

Tool cutting edge inclination λ_s = const. = −6°
Tool orthogonal rake angle γ_0 = const. = −6°

Tool	Tool corner radii r_ϵ [mm]	Applied cutting edge angles κ_r
T1	0.4; 0.8	95°
T2	0.8	50°; 95°
T3	0.8	95°

2.2. Analysis of fracture mechanisms

The broken chips were collected from the experiments and their fracture surfaces were investigated by scanning electron microscopy (SEM). Due to space limitations, Fig. 1 shows an exemplary fracture surface of *CuZn38As* (Tool T2, f = 0.30 mm; a_p = 1.6 mm, κ_r = 95°).

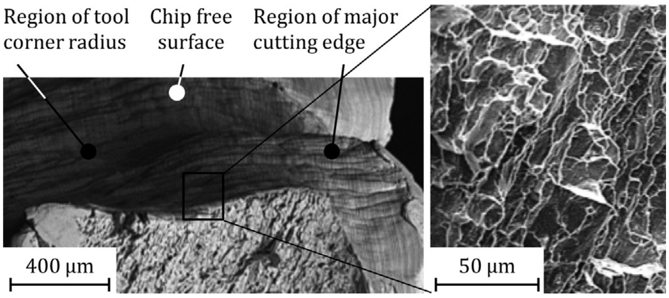

Fig. 1. Exemplary SEM images of ductile fracture surfaces.

The fracture surface shows a honeycomb-like structure, which is a characteristic indicator of ductile material fracture. It is also evident that the void-openings are oriented normal to the fracture surface, thus indicating the loading direction during the final chip breakage phase. This justifies modeling chip breakage for *AA7075-T6511* and *CuZn36As* materials as ductile fracture.

3. Predictive methodology for cutting tool and process design

3.1. Proposed methodology

Fig. 2 summarizes the proposed methodology for predictive tool and process design for stable chip breakage.

An initial cutting process is to be developed and optimized. First, the ductile fracture model is calibrated in a backward approach: In turning experiments, which can be conducted with arbitrary cutting conditions and tools, the helical geometry parameters of broken chips are measured. These are implemented into three earlier validated models, which calculate the distributions of equivalent strain ϵ_{eq}, temperature T, stress triaxiality η and Lode parameter $\bar{\Theta}$, under which ductile fracture was observed experimentally in the form of chip breakage [18–20]. The distributions are used to fit the material constants in the model for calculating the ductile fracture strain ϵ_f as follows:

$$\epsilon_f = \left[\left(D_1 \cdot e^{-D_2 \cdot \eta} - D_3 \cdot e^{-D_4 \cdot \eta}\right) \cdot \bar{\Theta}^2 + D_3 \cdot e^{-D_4 \cdot \eta}\right] \cdot \left[1 + D_5 \cdot \frac{T - T_0}{T_m - T_0}\right] \quad (2)$$

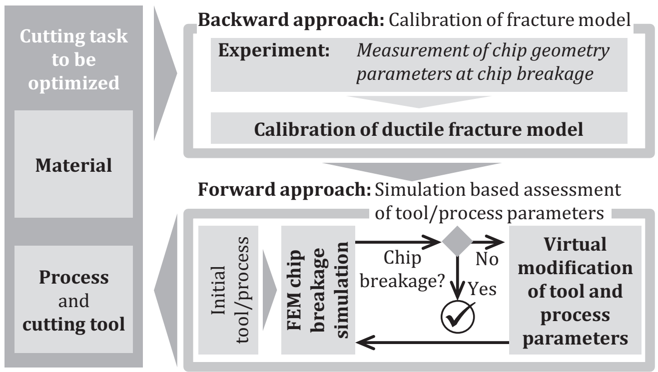

Fig. 2. Predictive methodology for tool and process design.

with D_1 to D_5 as material constants to be calibrated and T_0 and T_m as the reference and melting temperatures. A cutoff value for η of −1/3 was implemented by following previous work [17].

Afterwards, calibrated Eq. (2) is implemented into a 3D FEM model of the turning process during the Forward Approach. The initial cutting process is modified virtually. Only a limited number of cutting tests are necessary for the calibration of the fracture model. The methodology does not require any cost-intensive mechanical tests, which are usually necessary in order to calibrate stress-state and temperature-sensitive fracture models. The backward and